THE JOURNAL OF BIOLOGICAL CHEMISTRY VOL. 287, NO. 4, pp. 2500–2508, January 20, 2012

Core Fucosylation of μ Heavy Chains Regulates Assembly and Intracellular Signaling of Precursor B Cell Receptors*[S]

Received for publication, September 10, 2011, and in revised form, November 12, 2011 Published, JBC Papers in Press, November 14, 2011, DOI 10.1074/jbc.M111.303123

Wenzhe Li[‡1], Qingping Liu[‡], Yue Pang[‡], Jinhua Jin[‡], Huiguo Wang[‡], Hongyu Cao[‡], Zhi Li[§], Xu Wang[‡], Biao Ma[‡], Yan Chi[‡], Renjun Wang[‡], Akihiro Kondo[¶], Jianguo Gu[‖], and Naoyuki Taniguchi[**]

*From the [‡]Institute of Immunology, College of Life Science and Technology, Dalian University, 10-Xuefu Avenue, Dalian Economical and Technological Development Zone, Liaoning 116622, China, the [§]Clinical Laboratory, Dalian Central Hospital, 42 Xuegong Road, Shahekou District, Dalian City, Liaoning 116003, China, the [¶]Department of Molecular Diagnostics and Informatics, Osaka University Graduate School of Medicine, 1-7 Yamadaoka, Suita 565-0871, Japan, the [‖]Division of Regulatory Glycobiology, Institute of Molecular Biomembrane and Glycobiology, Tohoku Pharmaceutical University, 4-4-1 Komatsushima, Aoba-ku, Sendai, Miyagi 981-8558, Japan, and the **Systems Glycobiology Research Group, Advanced Science Institute, RIKEN, 2-1 Hirosawa, Wako, Saitama 351-0198, Japan*

Background: Formation of a functional precursor B cell receptor (pre-BCR) is dependent on *N*-glycosylation of μ-heavy chains (μHC).
Results: Lack of core fucosylation of μHC attenuated the interaction between μHC and λ5.
Conclusion: Core fucosylation of μHC mediates the assembly of pre-BCR.
Significance: Learning how Fut8 regulates the assembly of pre-BCR is crucial for understanding pre-B cell development.

α1,6-Fucosyltransferase (Fut8) knock-out (*Fut8*$^{-/-}$) mice showed an abnormality in pre-B cell generation. Membrane assembly of pre-BCR is a crucial checkpoint for pre-B cell differentiation and proliferation in both humans and mice. The assembly of pre-BCR on the cell surface was substantially blocked in the *Fut8*-knockdown pre-B cell line, 70Z/3-KD cells, and then completely restored by re-introduction of the *Fut8* gene to 70Z/3-KD (70Z/3-KD-re) cells. Moreover, loss of α1,6-fucosylation (also called core fucosylation) of μHC was associated with the suppression of the interaction between μHC and λ5. In contrast to *Fut8*$^{+/+}$ CD19^{+}CD43^{-} cells, the subpopulation expressing the μHC·λ5 complex in the *Fut8*$^{-/-}$ CD19^{+}CD43^{-} cell fraction was decreased. The pre-BCR-mediated tyrosine phosphorylation of CD79a and activation of Btk were attenuated in *Fut8*-KD cells, and restored in 70Z/3-KD-re cells. The frequency of CD19^{low}-CD43^{-} cells (pre-B cell enriched fraction) was also reduced in *Fut8*$^{-/-}$ bone marrow cells, and then the levels of IgM, IgG, and IgA of 12-week-old *Fut8*$^{-/-}$ mice sera were significantly lower than those of *Fut8*$^{+/+}$ mice. Our results suggest that the core fucosylation of μHC mediates the assembly of pre-BCR to regulate pre-BCR intracellular signaling and pre-B cell proliferation.

Early B lymphocytes in the bone marrow (BM)[2] can be divided into stepwise subsets from hematopoietic stem cells to mature B cells, based on the rearrangement of immunoglobulin genes and the expression of B cell receptor (BCR) and particular cell surface markers. The intermediate steps consist of pro-B cells (CD19^{+}CD43^{+} cells), in which the V(D)J rearrangement of the μ-heavy chain (μHC) gene is in process, and pre-B cells (CD19^{+}CD43^{-} cells), in which the gene rearrangement of light chains takes place. The first, critical checkpoint in early B lymphocyte development is transition from pro-B to pre-B cells. Only when the gene rearrangement of μHC is productive are pre-B cell antigen receptors (pre-BCR) expressed on their surface. A deficiency in pre-BCR formation results in severe impairment of B cell differentiation in both humans and mice (1). Thus, the early B-lymphocyte development relies on the assembly and expression of pre-BCR.

In a functional pre-BCR, immunoglobulin (Ig) μHC assembles with the surrogate light chain (SLC) and the signal-transducing heterodimer Igα/Igβ (CD79a and CD79b) (2, 3). The μHC (GI:90956) consists of the variable region of Ig HC (V_H) and the constant portion of the Ig HC (C_H). The SLC consists of 2 invariant polypeptides: λ5 (GI:54887631) and Vpre-B. Vpre-B and λ5 proteins are noncovalently associated and together form a SLC on the surface of B cell precursors. However, λ5 is covalently coupled to the C_H1 domain of μHC via a carboxyl-terminal cysteine (4).

GDP-L-Fuc:*N*-acetyl-β-D-glucosaminide α1,6-fucosyltransferase (Fut8) catalyzes the transfer of a fucose residue from GDP-fucose to the innermost *N*-acetylglucosamine (GlcNAc)

* This work was supported by National Nature Science Foundation of China Grant 30972675, the Scientific Research Foundation for the Returned Overseas Chinese Scholars, State Education Ministry (SRF for ROCS, SEM), and Science and Technology Planning Project of Dalian City, China, Grant 2010J21DW011.
[S] This article contains supplemental Figs. S1 and S2.
[1] To whom correspondence should be addressed: College of Life Science and Technology, Dalian University, 10-Xuefu Ave., Dalian Economical and Technological Development Zone, Liaoning 116622, China. Tel.: 86-411-87402337; Fax: 86-411-87403139; E-mail: liwenzhe46@hotmail.com.

[2] The abbreviations used are: BM, bone marrow; Fut8, core fucosyltransferase or α1,6-fucosyltransferase; pre-BCR, precursor B cell antigen receptor; μHC, μ heavy chain; SLC, surrogate light chain; VLA-4, very late antigen 4; AOL, *A. oryzae* lectin; GnTIII, *N*-acetylglucosaminyl transferase III; Btk, Bruton tyrosine kinase; 70Z/3-KD cell, *Fut8* knockdown 70Z/3 cell; 70Z/3-KD-re cell, *Fut8* restored 70Z/3-KD cells; PE, phycoerythrin.

residue of hybrid and complex *N*-glycans via an α1,6-linkage (core fucosylation) in the Golgi apparatus in mammals (5) as shown in supplemental Fig. S1. The presence of core fucose in the *N*-linked glycoprotein has been shown to be important in glycoprotein processing and recognition. A lack of core fucosylation of the transforming growth factor-β1 (TGF-β1) receptor and/or epidermal growth factor (EGF) receptor consequently results in the marked dysregulation of their activation, due to a decreased ligand affinity for the receptor (5–7). Deletion of the core fucose from the Cγ2 of IgG_1 enhanced antibody-dependent cell-mediated cytotoxity up to 50–100-fold (8). Recently, Pinho *et al.* (9) reported that the modification of *Fut8* on E-cadherin affected the adhesive function of this adhesion molecule. More recently, it has been reported that *Fut8*$^{-/-}$ mice exhibited multiple behavioral abnormalities associated with a schizophrenia-like phenotype (10). Taken together, these results suggest that the core fucose plays a key role in regulating important physiological functions via the modification of functional proteins.

The μHC is a glycoprotein, containing 5 potential *N*-glycosylation sites: N^{46} (C_H1), N^{211} (C_H2), N^{243} (C_H3), N^{258} (C_H3), and N^{281} (C_H3) in mice (11). It has been reported that *N*-glycosylation of IgM was related to serum half-life, complement activation, and IgM oligomerization (12, 13). Haimovich *et al.* (14) demonstrated that *N*-glycosylation in μHC plays a role in its activation. Recently, Ubelhart *et al.* (11) also reported that the formation of a functional pre-BCR was strictly dependent on a specific *N*-glycosylation site in the C_H1 domain of μHC. The core fucose is present in several classes of *N*-linked glycans and could affect the conformation and flexibility of the antenna of *N*-linked biantennary oligosaccharides (15). However, the role of core fucosylation of μHC in pre-BCR assembly has not yet been addressed.

In our previous study, the loss of core fucosylation of very late antigen 4 and vascular cell adhesion molecule 1 led to the low interaction between pre-B cells and stromal cells, which accounts for an abnormality in the development of B cell progenitors (16). In the present study, we further explored a new mechanism of B lymphopoietic failure at the pre-B cell stage in *Fut8*$^{-/-}$ mice, and found that core fucosylation of μHC was required for the assembly of pre-BCR and intracellular signaling via pre-BCR.

EXPERIMENTAL PROCEDURES

Mice—Fut8$^{-/-}$ mice were generated as previously described (6) and were backcrossed eight times to the BALB/cA background. Homozygous wild (*Fut8*$^{+/+}$) and knock-out (*Fut8*$^{-/-}$) mice were obtained by crossing heterozygous *Fut8*$^{+/-}$ mice. All animal procedures complied with the institutional animal protocol guidelines. Peripheral blood was collected by cardiac puncture. The component of peripheral blood was analyzed by the Research Foundation for Microbial Diseases of Osaka University.

Antibodies—FITC-labeled anti-IgM (II/41), anti-erythroid (TER-119), anti-CD79b (HM79-16), PE-labeled anti-CD43 (S7), anti-IgD(11–26), PE-Cy5-labeled anti-CD19 (MB19-1), anti-Gr-1 (RB6–8C5), and APC-labeled anti-CD11b (Mac-1, M1/70) and anti-CD45R (RA3–6B2) monoclonal antibody (mAb) were obtained from e-Bioscience. Biotin-conjugated anti-mouse pre-BCR mAb (SL156), streptavidin-PE Cy5, and λ5 (LM34) were purchased from BD Bioscience. Anti-phosphotyrosine antibody (Ab) (PY20) was from BD Transduction Laboratories. Abs specific to Vpre-B (M-17; sc-25014), rat/mouse β-actin (sc-8432), was purchased from Santa Cruz; anti-mouse CD79a mAb were obtained from Beckman-Coulter-Immunotech. A mouse anti-Fut8 mAb (15C6) was obtained from Fujirebio Inc. (Japan); a rabbit anti-mouse IgG HRP-conjugate was from ICN Pharmaceuticals, Inc. (Aurora, OH). The anti-μHC mAb was from Southern Biotech.

Cells and Culture Conditions—The 70Z/3 cells, a pre-B lymphoma line, were purchased from ATCC. 70Z/3 derivative cell lines, stably transfected with the pSINsi-mU6 plasmid expressing siRNA that targeted *Fut8* are referred to hereafter as "70Z/3-KD." *Fut8* restored 70Z/3-KD cells, 70Z/3-KD-re cells were established as previously described (16). The cells were grown in RPMI 1640 supplemented with 2 mM glutamine, 50 μM 2-mercaptoethanol (Fluka, Buchs, Switzerland), 5% FCS, 100 units/ml of penicillin, 100 μg/ml of streptomycin.

Flow Cytometry and Cell Sorting—BM cells and 70Z/3 cells in subconfluent conditions were harvested using phosphate-buffered saline (PBS) containing 0.2% EDTA and centrifuged at 1,000 × *g* for 5 min. The cell pellets were suspended in PBS(−) (5×10^6 cells) and incubated with an anti-CD16/CD32 (2.4G2) mAb to block Fc receptors and then stained on ice for 15 min with several combinations of mAbs, as indicated in the figure legends. Flow cytometry was performed on a FACS-Calibur (BD Biosciences), and the data were analyzed with CellQuest (BD Biosciences).

For cell sorting, BM cells were obtained by crushing two femurs and two tibia of 1-week-old mice. The crude mixture was filtered through nylon mesh, and resuspended at 1×10^7 cells/ml. BM cells were stained with PE-labeled anti-CD43 Ab and PE-Cy5-labeled anti-CD19 Ab and subpopulations were sorted with a FACStar Plus (BD Biosciences) instrument.

Fut8 Enzyme Activity Assay—The enzyme activity of Fut8 was determined using a synthetic substrate, 4-(2-pyridylamino)butylamine-labeled oligosaccharide as a substrate. Cells grown to subconfluence were washed with PBS(−) once, and the cell pellet was suspended in 200 μl of lysis buffer containing 10 mM Tris-HCl (pH 7.4), 150 mM NaCl, and 1% Triton X-100. The cell lysate was then assayed for Fut8 activity by high-performance liquid chromatography (HPLC) as described previously (17).

Western Blot and Lectin Blot Analysis—Cells were solubilized in 1% Triton X-100 lysis buffer (20 mM Tris-HCl (pH 7.4), 10 mM EGTA, 10 mM $MgCl_2$, 1 mM benzamidine, 60 mM β-glycerophosphate, 1 mM Na_3VO_4, 20 mM NaF, 2 μg/ml of aprotinin, 5 μg/ml of leupeptin, 0.1 mM phenylmethylsulfonyl fluoride) and then centrifuged at 15,000 × *g* for 15 min. The supernatants were collected, and protein concentrations were determined using a protein assay BCA kit (Pierce). Equal amounts of protein were run on 10% SDS-PAGE under reducing conditions and then transferred to PVDF membranes (Millipore Corp.). Blots were blocked for 2 h with 5% skim milk in TBS-T (TBS-T; 10 mM Tris-HCl (pH 7.5), 150 mM NaCl, and 0.1% Tween 20) for immunoblot or with 3% BSA in TBS-T for lectin blot. Fol-

lowing incubation with the appropriate primary antibodies or 0.5 μg/ml of biotin-conjugated *Aspergillus oryzae* lectin (AOL) (18), which preferentially recognizes core fucosylation on *N*-glycans overnight, and then the membranes were washed. After washing, the blots were incubated with the corresponding secondary antibodies conjugated with horseradish peroxidase or ABC reagent (Vector Laboratories) for the AOL blot. Finally, specific proteins were visualized using an ECL system (Amersham Biosciences). These membranes were stripped and reprobed with an antibody against the corresponding total proteins to confirm equal loading.

Cell Surface Biotinylation and Immunoprecipitation—Cells were surface labeled by a sulfosuccinimido-biotin (sulfo-NHS-biotin) (Pierce) procedure (19). Briefly, after three washes the cells were suspended in PBS with 0.2 mg/ml of sulfo-NHS-biotin. After a 1-h incubation at 4 °C with occasional shaking, the cells were washed three times with chilled PBS and solubilized in lysis buffer.

Cell lysates (about 500 μg of protein) were incubated with the indicated antibodies overnight at 4 °C with gentle rocking and then added to 20 μl of protein G-Sepharose (50% slurry) (Amersham Biosciences) for another incubation of 2 h at 4 °C. The immunoprecipitate was washed three times with lysis buffer. The biotinylated proteins were visualized using the Vectastain ABC and ECL kits.

Assays for Frequencies of Pre-B Cells—The frequencies of pre-B cells growing dependent on SL156 plus interleukin 7 (IL-7) (clonable pre-B cells) were evaluated by means of a clonable pre-B cell assay with some modifications (16). The enriched $CD19^{low}CD43^-$ cells were seeded into methylcellulose media containing 10 ng/ml of recombinant human IL-7 (Stemcell Technologies Inc.) and 10 ng/ml of SL156. Colonies were counted after 7 days of culture. Aggregates consisting of >40 cells were differentially scored as colonies. All assays were performed in triplicate.

Assay for Molecular Interaction—Real-time molecular analysis was performed with an optical biosensor (Affinity Sensors, Cambridge, UK). Biotinylated λ5 peptide (NH_2-wyvfgggtqltilgqpksdplvtlflpslknlqptrphvvclvsefypgtlvvdwkvdgvpvtqgvettqpskqtnnkymvssyltlisdqwmphsryscrvthegntveksvspaecs-COOH) was obtained by solid synthesis (Takara Bio). The biotinylated λ5 was immobilized on a biotinyl cuvette via streptavidin. Then, various concentrations of μHC purified from the lysates of 70Z/3, 70Z/3-KD, and 70Z/3-KD-re cells were placed in the cuvette.

Real-time PCR—Real-time PCR analyses were performed using a Smart Cycler II System (Cephied, Sunnyvale, CA) as described (6, 18).

Enzyme-linked Immunosorbent Assay (ELISA) for Immunoglobulin Typing—ELISA was carried out using mouse monoclonal antibody isotyping reagents (Sigma). The sera from 2- and 12-week-old mice (three per group) were used in this experiment.

Statistical Analysis—The results are expressed as mean ± S.D. Statistical analyses were carried out using Student's *t* test. A *p* value of less than 0.05 was considered statistically significant.

TABLE 1
Comparison of BM cell compositions between *Fut8*$^{+/+}$ and *Fut8*$^{-/-}$ mice
Data are representative of the mean ± S.D. of four mice per genotype.

Genotype	*Fut8*$^{+/+}$ mice	*Fut8*$^{-/-}$ mice	*p* values
WBC (10^6/ml)	3.8 ± 1.2	2.7 ± 0.7	$0.01 < p < 0.05$
$CD19^+CD45R^+$ (%)	36.5 ± 2.6	16.2 ± 2.6	$p < 0.01$**
$CD19^+CD43^+$ (%)	5.9 ± 1.6	5.2 ± 2.1	$p > 0.05$
$CD19^+CD43^-$ (%)	30.2 ± 4.6	10.8 ± 5.5	$p < 0.01$**
$CD19^+IgM^+$ (%)	6.8 ± 1.7	3.7 ± 1.1	$0.01 < p < 0.05$
$CD11b^+Gr\text{-}1^-$ (%)	4.9 ± 3.4	7.9 ± 1.5	$0.01 < p < 0.05$
$TER119^+$ (%)	30.5 ± 3.5	47.7 ± 2.1	$p < 0.01$**
$DX5^+CD3^-$ (%)	1.1 ± 0.3	1.2 ± 0.5	$p > 0.05$
$DX5^+CD3^+$ (%)	0.8 ± 0.5	0.9 ± 0.2	$p > 0.05$
IgM^+CD5^+ (%)	1.8 ± 1.0	1.7 ± 1.2	$p > 0.05$

RESULTS

Impaired Pre-B Cell Population in Fut8$^{-/-}$ *BM Cells*—To determine the effects of targeting *Fut8* on the hematolymphopoietic system, we analyzed peripheral blood cells of *Fut8*$^{-/-}$ mice. In the peripheral blood test, the numbers of white blood cells (WBC) in *Fut8*$^{-/-}$ mice were 2.7 ± 0.7 × 10^6/ml, whereas those in *Fut8*$^{+/+}$ mice were 3.8 ± 1.2 × 10^6/ml (Table 1). Because the Fut8 product, a core-fucosylated *N*-glycan, is ubiquitously expressed in the BM microenvironment of *Fut8*$^{+/+}$ BM, as confirmed by fucose lectin, AOL (16), a decrease of peripheral white blood cells in *Fut8*$^{-/-}$ mice suggest that Fut8 plays some positive roles in the regulation of hematopoiesis in the BM. Flow cytometry analysis revealed that the population of $CD45^+CD19^+$ cells was markedly reduced in *Fut8*$^{-/-}$ BM (Fig. 1 and Table 1). Also, the $CD19^+CD43^-$ (pre-B enriched) and $CD19^+IgM^+$ (immature B enriched) populations were significantly decreased in *Fut8*$^{-/-}$ BM, whereas the $CD19^+CD43^+$ (pro-B enriched) population was sustained (Fig. 1 and Table 1). The populations of $CD11b^+$ myeloid cells and $TER119^+$ erythroid cells were relatively increased in *Fut8*$^{-/-}$ BM (Fig. 1 and Table 1), probably reflecting the reduction of B-lineage fractions. Development of B-1 cells, natural killer cells, and natural killer T cells were relatively normal in *Fut8*$^{-/-}$ BM (Table 1). Our results showed that disruption of *Fut8* led to an abnormality in the development of the pre-B cell stage.

Membrane Assembly of Pre-BCR Requires μHC Core Fucosylation—In our previous study, we established *Fut8* knockdown 70Z/3 cells, namely 70Z/3-KD cells, and *Fut8* restored 70Z/3-KD cells (70Z/3-KD-re cells) (16). As shown in Fig. 2*A*, the expression of *Fut8* mRNA was significantly reduced in 70Z/3-KD cells, and then re-introduction of the *Fut8* gene into 70Z/3-KD cells resulted in recovery of *Fut8* expression. Again, Fut8 enzyme activity analysis reflected the results of *Fut8* gene expression. Fut8 activities were barely detectable in 70Z/3-KD cells, and were restored in 70Z/3-KD-re cells (Fig. 2*B*). Again, an AOL blot analysis reflected the results of the mRNA expressions and enzyme activities (supplemental Fig. S2), suggesting that the post-translational modification by core fucosylation on *N*-glycans is only catalyzed by the *Fut8* gene. No apparent changes were found in the expressions of other glycosyltransferase genes, such as *GnT*III and *β4GalT*-I (Fig. 2*C*).

Membrane assembly of the pre-BCR is a crucial checkpoint for B cell differentiation and proliferation in both humans and mice (20–23). The μHC produced by pre-B cells performs a

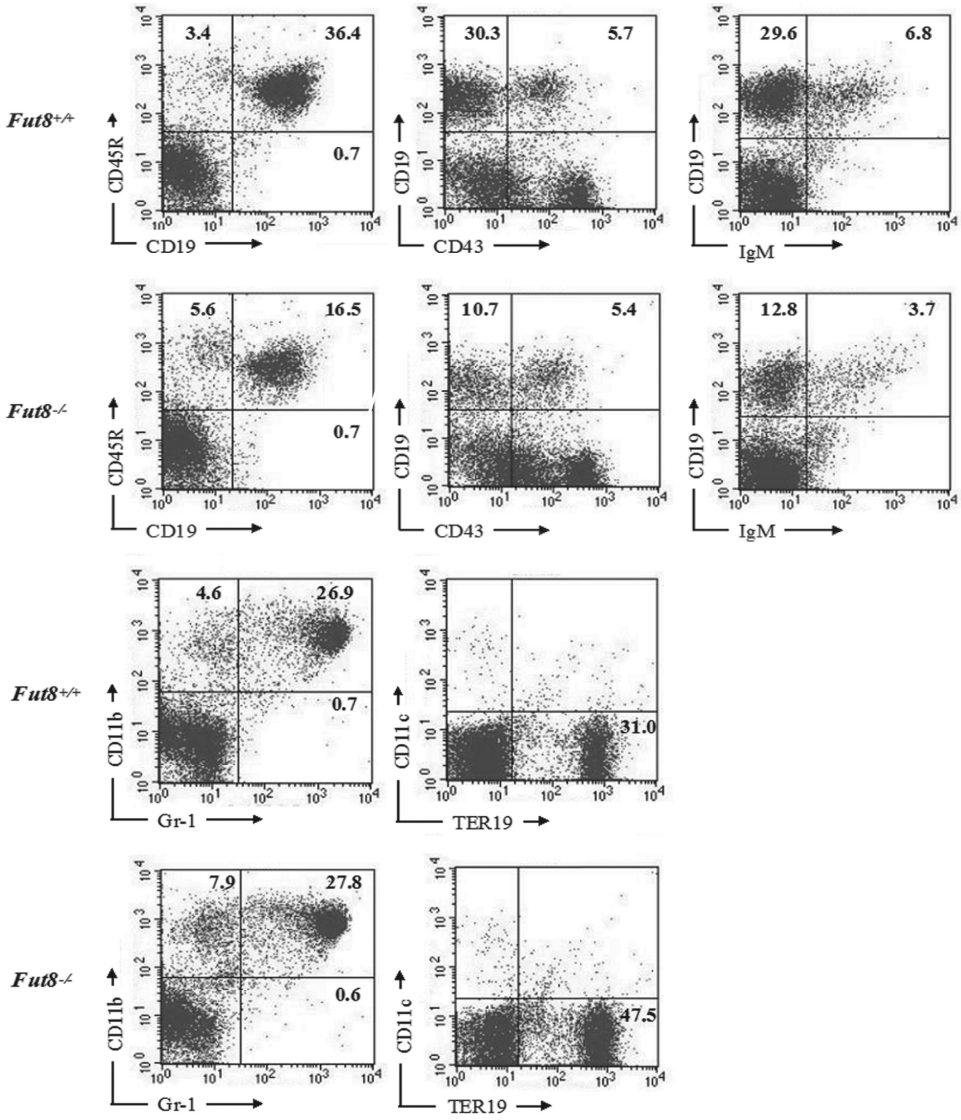

FIGURE 1. **FACS analysis of the proportion of CD45R$^+$CD19$^+$, CD19$^+$CD43$^-$, CD19$^+$CD43$^+$, CD19$^+$IgM$^-$, CD19$^+$IgM$^+$, CD11b$^+$, CD11c$^+$, Gr-1$^+$, and TER119$^+$ cells in *Fut8*$^{-/-}$ BM.** BM cells were obtained by crushing 2 femurs and 2 tibia of 1-week-old mice. The crude mixture was filtered through nylon mesh, and resuspended at 1×10^7 cells/ml. *Upper panels* indicate *Fut8*$^{+/+}$ BM cell subsets and the *lower panels* indicate *Fut8*$^{-/-}$ BM cell subsets. *Numbers* indicate the percentage of the total BM cells within this quadrant, and 10,000 events were acquired for each analysis. The results of 1 of 4 representative experiments are shown.

very important role to form the pre-BCR, which is composed of μHC and SLC (22). The C_H1 of μHC reportedly contained the *N*-linked glycosylation site N^{46}, and the conserved N^{46}-glycosylation site is important for pre-BCR function (11). To elucidate the effects of core fucosylation in the assembly of pre-BCR, we examined the expression level of pre-BCR on the cell surface by biotin labeling. As shown in Fig. 3*A*, the expression of pre-BCR on the cell surface was down-regulated in 70Z/3-KD, and was restored in 70Z/3-KD-re cells. In the densitometric analysis, in contrast to 70Z/3 cells, pre-BCR expression on the cell surface was down-regulated by a factor of 5.2 in 70Z/3-KD cells. However, no significant differences in the expression levels of intracellular precursor μHC were found among the 3 cell types (Fig. 3*B*). The levels of core fucosylation in μHC were abolished in 70Z/3-KD cells, and they were rescued by reintroduction of *Fut8* (Fig. 3*B*), suggesting that μHC is the target of *Fut8*. In the immunoprecipitation assay, we also found that loss of core fucosylation of μHC impaired the interaction between μHC and λ5, but not between μHC and Vpre-B (Fig. 3*C*). There were no differences in the expression levels of λ5 among the 3 cell types. Because λ5 is covalently coupled to the C_H1 domain of μHC via a carboxyl-terminal cysteine (4), we synthesized a peptide, the COOH-terminal portion of λ5, and detected the binding affinity of λ5 to μHC. In the binding assay using an optical biosensor IAsys, the purified μHC from 70Z/3-KD cells showed impaired adhesion to the synthetic λ5 peptide (0.05, 0.1, and 0.2 μM), by comparison with mock cells. The reintroduction of *Fut8* restored the binding affinity of μHC to λ5 (Fig. 3*D*). These results indicated that core fucosylation of μHC is required for the functional interaction between μHC and λ5 to complete the assembly of the pre-BCR.

Next, we examined the surface expressions of μHC, λ5, pre-BCR, and CD79b on CD19$^+$CD43$^-$ cells (enriched pre-B) by flow cytometry. Pre-B cells express cell surface CD19 and cell

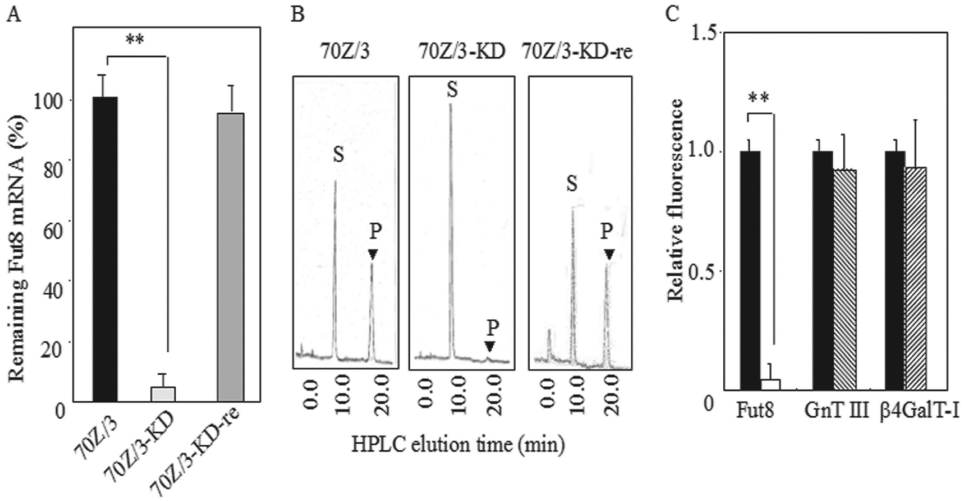

FIGURE 2. **Characterization of 70Z/3-KD and 70Z/3-KD-re cells.** *A,* gene-silencing effects of siRNA on the *Fut8* mRNA expression were determined by real-time PCR, and normalized by the levels of GAPDH ($n = 3$). *B,* analyses of Fut8 activity. Fut8 activity was examined using a fluorescence-labeled sugar chain, GnGn-Asn-PABA (4-(2-pyridylamino)butylamine), as an acceptor substrate, as described under "Experimental Procedures." The substrate (*S*) and Fut8 product (*P*) were eluted at 10 and 20 min, respectively, in mock and restored cells but not in 70Z/3-KD cells. *ND*, not detectable. Restored, re-introduction of *Fut8* gene into 70Z/3-KD cells. *C,* gene expressions of Fut8, GnTIII, and β4GalT-I by real-time PCR analysis. RNAs were isolated from 70Z/3 and 70Z/3-KD cells. All values were normalized to that of the *GAPDH* gene. 70Z/3-KD cell, *Fut8* knockdown 70Z/3 cell; 70Z/3-KD-re cell, *Fut8* restored 70Z/3-KD cells. Data were representative of the mean ± S.D. of 3 per genotype (**, $p < 0.01$).

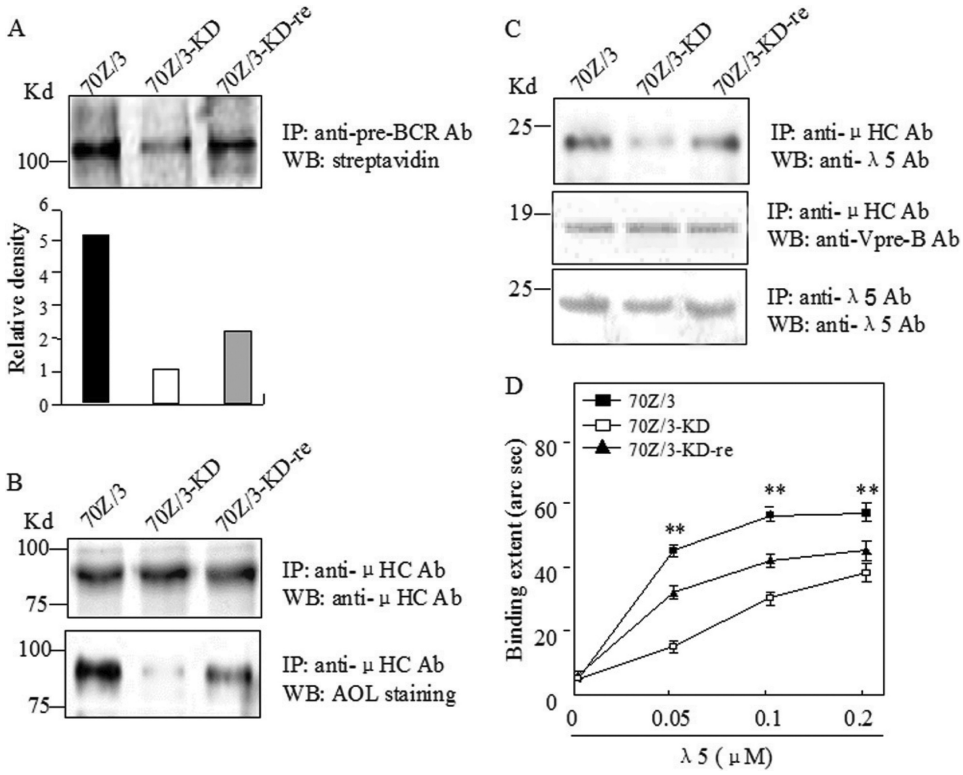

FIGURE 3. **Membrane assembly of pre-BCR requires μHC core fucosylation.** *A,* cell surface biotinylation and immunoprecipitation of pre-BCR from 70Z/3, 70Z/3-KD, and 70Z/3-KD-re cells. The surface cellular proteins of the indicated cells were biotinylated before cell lysis. Whole lysates were immunoprecipitated (*IP*) with anti-pre-BCR antibody. The samples were subjected to 10% SDS-PAGE. After Western blotting (*WB*), the membrane was incubated with streptavidin-HRP. Quantification of expression levels of pre-BCR was analyzed by NIH Image 1.63. *B,* core defucosylation of μHC in 70Z/3-KD cells. The cell lysates were immunoprecipitated by anti-μHC Ab, and the immunoprecipitates were resolved by SDS-PAGE on 7.5% gel, transferred to a PVDF membrane, and probed with the anti-μHC Ab (*upper panel*) and AOL (*lower panel*). Abrogation of the core fucose of μHC was detected by AOL staining. *C,* impaired interaction between μHC and λ5 in 70Z/3-KD cells. Cell lysates were immunoprecipitated with anti-μHC Ab and analyzed by Western blot with antibody to λ5 (*upper panel*) and cell lysates were immunoprecipitated with anti-λ5 Ab and analyzed by Western blot with antibody to λ5 (*lower panel*). *D,* molecular interactions between λ5 and μHC, detected by an optical biosensor ($n = 3$). The μHCs were extracted from the lysates of 70Z/3, 70Z/3-KD, and 70Z/3-KD-re cells. Monobiotinylated λ5 were coated. The data reflect the proportion of μHC associated with λ5.

surface μHCs associated with SLCs, whereas Pro-B cells are those B-lineage cells that express cell surface CD19 but do not express cytoplasmic or cell surface μHCs (28). In contrast with *Fut8*$^{+/+}$ CD19^{+}CD43^{-} cells, the subpopulation expressing the μHC·λ5 complex in the *Fut8*$^{-/-}$ CD19^{+}CD43^{-} cell fraction was significantly decreased (Fig. 4). The percentage of *Fut8*$^{-/-}$

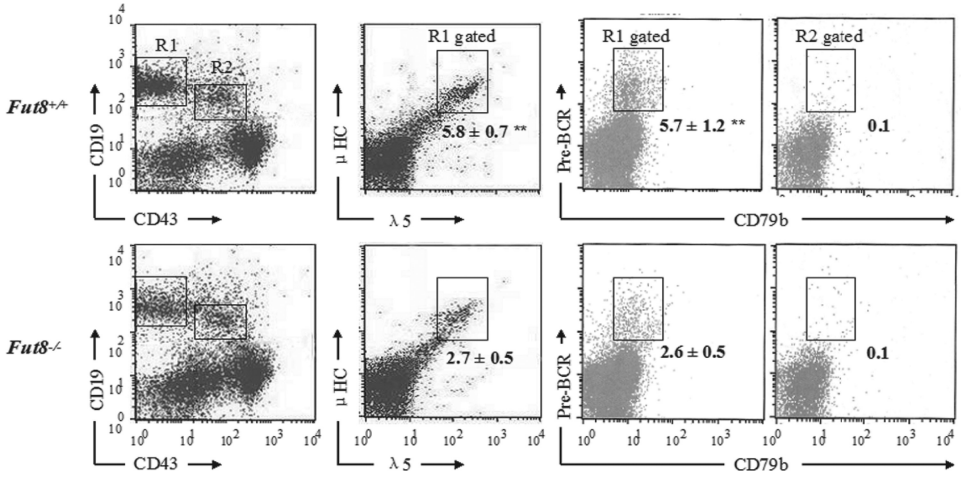

FIGURE 4. **Impaired generation of $\mu HC^{+}\lambda5^{+}$ cells and pre-$BCR^{+}CD79b^{low}$ in *Fut8*$^{-/-}$ $CD19^{+}CD43^{-}$ pre-B cells.** $CD19^{+}CD43^{-}$ pre-B cells (*R2*) and $CD19^{+}CD43^{+}$ pro-B cells (*R1*) were gated. *Upper panels* indicate *Fut8*$^{+/+}$ cell subsets and *lower panels* indicate *Fut8*$^{-/-}$ cell subsets. *Numbers* adjacent to the *boxed areas* indicate the frequency of $\mu HC^{+}\lambda5^{+}$ cells and pre-$BCR^{+}CD79b^{low}$ cells in each as a percentage of the total cells. Data were representative of the mean ± S.D. of 3 per genotype (**, $p < 0.01$). Data were analyzed using the FLOWJO software program.

pre-$BCR^{+}CD79b^{low}$ cells was 2.6 ± 0.5% of the pre-B cells ($CD19^{+}CD43^{-}$ cells), whereas that of *Fut8*$^{+/+}$ pre-$BCR^{+}CD79b^{low}$ cells was 5.7 ± 1.2% (Fig. 4). No expression of either pre-BCR or CD79b was found in $CD19^{+}CD43^{+}$ cells (enriched pro-B). These results suggested that inefficient assembly of the pre-BCR due to core defucosylated μHC accounted for low levels of pre-BCR expression on the *Fut8*$^{-/-}$ and *Fut8* knockdown cell surface.

Loss of Fut8 Reduced Transduction of Pre-BCR Signaling—Signaling events initiated by the pre-BCR regulate several biological functions including cell proliferation and differentiation (4). The monoclonal antibody SL156 is specific for total pre-BCR and could cross-link the pre-BCR on the cellular surface to induce sustained intracellular signaling (37). Pre-BCR activation begins by the phosphorylation of the immunoreceptor tyrosine-based activatory motif present on the cytoplasmic tails of the CD79a and CD79b molecules and relies on the sequential activation of Src protein-tyrosine kinases Lyn, Syk, and the Bruton tyrosine kinase (Btk) (24). To address the effects of core fucosylation in pre-BCR mediated signaling, the cells were stimulated by SL156, and then the cell lysates were immunoprecipitated with anti-CD79a antibody. The kinetics of CD79a phosphorylation were quite similar in the 3 cell lines, and reached the maximal level at 5 min and returned to the basal level within 15 min after the stimulation of monoclonal antibody SL156. However, compared with 70Z/3 cells, the phosphorylation level of CD79a at 5 min was attenuated by a factor of 6.7 in 70Z/3-KD cells, whereas down-regulation of phosphorylation was partly restored in 70Z/3-KD-re cells (Fig. 5*A*). Moreover, the expression level of CD79a was reduced in 70Z/3-KD cells, compared with 70Z/3 and 70Z/3-KD-re cells (Fig. 5*A*). Also, the phosphorylation of Btk at 15 min was reduced by a factor of 3.8 in 70Z/3-KD cells, whereas those of Btk were rescued in the 70Z/3-KD-re cells (Fig. 5*B*). It is noteworthy that incomplete pre-BCR complex formation was seen in *Fut8*$^{-/-}$ mice, which were expected to have compromised signaling capacity.

Loss of Fut8 Reduced Frequency of Pre-B Cells and Production of IgM, IgA, and IgG—To determine whether the core-fucosylated *N*-glycans functionally compromised pre-B cell colony formation, we cultivated 70Z/3, 70Z/3-KD, and 70Z/3-KD-re cells in Complete methylcellulose medium in the presence of SL156 plus IL-7. In the 70Z/3-KD cells the frequency of clonable pre-B cell progenitors was decreased, in comparison with mock cells and 70Z/3-KD-re cells (Fig. 6*A*). Moreover, colony formation of *Fut8*$^{-/-}$ $CD19^{low}CD43^{-}$ cells (pre-B cell enriched) were suppressed, compared with those of *Fut8*$^{+/+}$ $CD19^{low}CD43^{-}$ cells (Fig. 6*B*). Our previous study showed that colony formation of pre-B cells in Complete methylcellulose medium in response to IL-7 alone (CFU-IL-7) was indistinguishable between *Fut8*$^{+/+}$ pre-B cells and *Fut8*$^{-/-}$ pre-B cells (16), indicating that core fucosylation is critically important for pre-BCR-dependant cell proliferation.

We further examined the amount of each immunoglobulin isotype by ELISA. In 2-week-old *Fut8*$^{-/-}$ mice, the levels of IgM and IgG3 were significantly lower than those in *Fut8*$^{+/+}$ mice, whereas the amounts of other immunoglobulins, IgG_1, IgG_{2a}, IgG_{2b}, and IgA, were relatively normal. However, in 12-week-old *Fut8*$^{-/-}$ mice sera, the levels of IgG_1, IgG_{2a}, IgG_{2b}, IgA, IgG3, and IgM were significantly reduced (Fig. 7). These data indicate that *Fut8*$^{-/-}$ mice exhibited defective humoral immune responses in addition to impaired early B cell development, in transition from pro-B to pre-B cells.

DISCUSSION

A selective and profound reduction in the pre-B cell populations and no concomitant change in the population containing pro-B cells were observed in *Fut8*$^{-/-}$ BM (Fig. 1 and Table 1). In agreement with this result, in 70Z/3-KD cells, the frequency of clonable pre-B cell progenitors was reduced, compared with mock cells and 70Z/3-KD-re cells. The present study is the first to clearly demonstrate that core fucosylation of μHC influences the pre-BCR assembly so as to regulate pre-BCR signaling and pre-B cell proliferation.

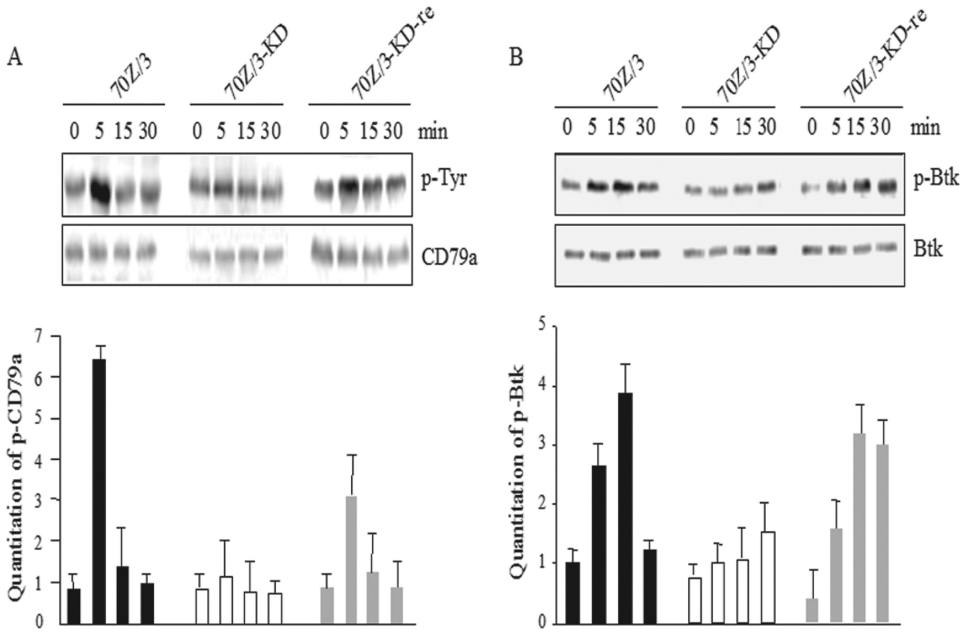

FIGURE 5. **Down-regulation of phosphorylated CD79a and Btk in 70Z/3-KD cells.** The serum-starved cells of 70Z/3, 70Z/3-KD, or 70Z/3-KD-re were treated with anti-pre-BCR antibody (SL156) at the indicted concentrations for 5 min and solubilized in lysis buffer as described under "Experimental Procedures." Whole cell lysates were subjected to 10% SDS-PAGE. *A*, protein expression and phosphorylated forms of CD79a. The cell lysates were immunoprecipitated by anti-CD79a Ab, and the immunoprecipitates were resolved by SDS-PAGE on a 7.5% gel, transferred to a PVDF membrane, and probed with the PY20 (*upper panel*) and CD79a (*lower panel*). Increased phosphorylation of CD79a was maximal by 5 min. The quantitative data of phosphorylated CD79a were represented as the mean ± S.D. ($n = 3$). *B*, protein expression and phosphorylated forms of Btk are indicated in Western blot. The blots were probed with anti-*p*-Btk Ab (*upper panel*) or anti-Btk Ab (*lower panel*). The quantitative data of phosphorylated Btk are represented as mean ± S.D. ($n = 3$).

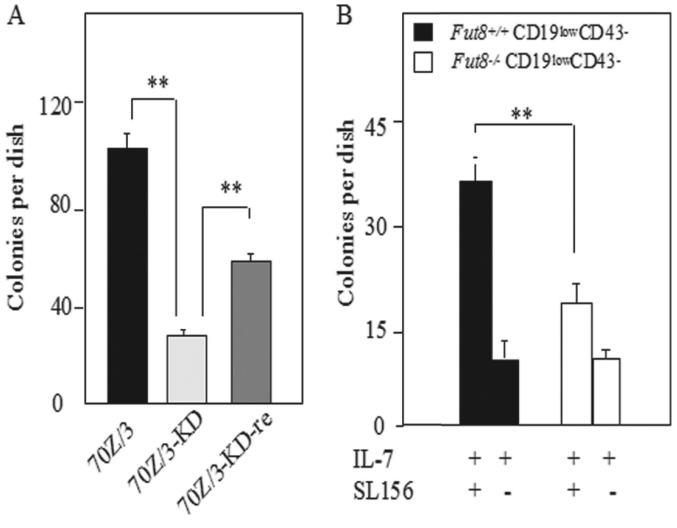

FIGURE 6. **The pre-B colonies in the Complete methylcellulose medium in the presence of SL156 and IL-7.** *A*, comparison of the frequencies of 70Z/3, 70Z/3-KD, and 70Z/3-KD-re cells in response to SL156 + IL-7. *B*, comparison of the frequencies of pre-B cells between *Fut8*$^{+/+}$ CD19^{low}CD43^{-} and *Fut8*$^{-/-}$ CD19^{low}CD43^{-} cells in response to SL156 and IL-7. CD19^{low}CD43^{-} pre-B cells were isolated using a FACStar Plus (BD Biosciences) instrument. Sorted cell populations were routinely re-analyzed and showed more than 92% purity. The pre-B colonies counted were cultured for 7 days in Complete methylcellulose medium in the presence of SL156 and IL-7. Data are presented as mean ± S.D. of pre-B colony-forming units.

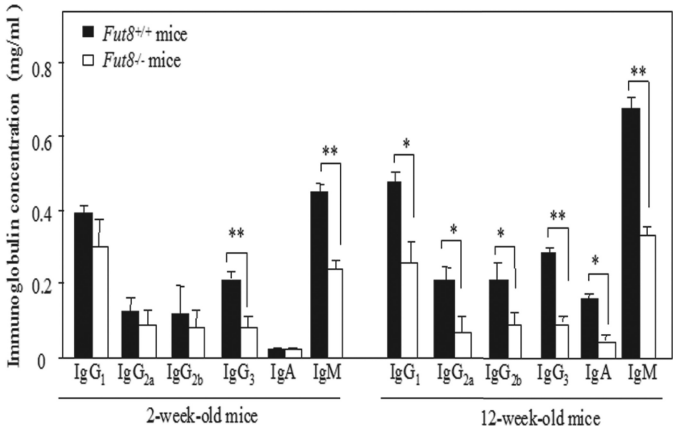

FIGURE 7. **Comparison of the levels of serum immunoglobulin isotypes in *Fut8*$^{+/+}$ and *Fut8*$^{-/-}$ mice.** The sera from 2- and 12-week-old mice (three per group) are used in this experiment. The concentrations of immunoglobulin isotypes are measured by ELISA kit (Sigma). ELISA was carried out using mouse monoclonal antibody isotyping reagents. **, $p < 0.01$ and *, $p < 0.05$ were considered statistically significant.

It is well known that glycoprotein expression can be regulated at post-translational levels. The mammalian glycans produced in the Golgi modulate the endocytosis of cell-surface glycoproteins, thereby controlling protein expression (25–27). The μHC have been described through the Golgi system, and are transported to the cell surface after modification of the carbohydrate moieties (28). The μHCs associated with the SLC were typically obligatory for pre-BCR transport to the surface (29–31). λ5 is covalently coupled to the C_H1 domain of μHC via a carboxyl-terminal cysteine (4). λ5 has no potential *N*-glycosylation sites, whereas the C_H1 domain of μHC has a single *N*-glycosylation site, N^{46}. Ubelhart *et al.* (11) also found that a conserved N^{46}-glycosylation site in the C_H1 domain of μHC was the crucial element that regulates the interaction of μHC and λ5, followed by pre-BCR formation. Fut8 could modify multiple proteins and the core fucosylation of protein is an important post-translational process, which regulates protein folding, stability, and functional expression (5–10). To investi-

gate an abnormality in pre-B cell development in *Fut8*$^{-/-}$ mice, here, we focused only on the role of core-fucosylated μHC during the assembly of pre-BCR. As anticipated, loss of core fucosylation of μHC impaired the interaction between μHC and λ5 (Fig. 3, *C* and *D*). The formation of pre-BCR on the cell surface was down-regulated in 70Z/3-KD, and was restored in 70Z/3-KD-re cells (Fig. 3*A*). This notion was also supported by evidence showing that in *Fut8*$^{-/-}$ BM the subpopulation of μHC^{+}λ5^{+} cells was lower than *Fut8*$^{+/+}$ BM. Indeed, not all rearranged μHCs can pair with the SLC to form a pre-BCR: only half of the in-frame rearranged μHCs pair correctly with SLCs (32). Only those B cells that express a μHC capable of pairing with an SLC undergo clonal expansion. Because the core fucosylation of μHC is required for the assembly of pre-BCR (11), and because the expression of the *Fut8* gene was dramatically up-regulated at the developmental stage from pro-B to pre-B cells (16), it is conceivable that *Fut8* regulates the level of core fucosylation of μHC, followed by assembly of pre-BCR and B cell clonal expansion. In addition to interaction between λ5 and the C_H1 domain of μHC, in a pre-BCR complex, the interaction occurs between Vpre-B and the V_H domain. Indeed, the Vpre-B is stabilized by a salt bridge between Vpre-B residue Glu^{106} and V_H residue Arg^{59} (3). The V_H domain, Vpre-B, and λ5 do not have any potential *N*-glycosylation sites, the interaction between the V_H domain of μHC and Vpre-B belongs to the protein-protein interaction, whereas the interaction between the C_H1 domain of μHC and λ5 is a protein-glycoprotein interaction. It is reasonable that the loss of core fucosylation of the C_H1 domain of μHC could suppress the interaction between C_H1 and λ5, but could not influence the formation of a salt bridge between the Vpre-B and the μHC.

The pro-B/pre-B I cells, freshly isolated from the BM, are able to differentiate and divide 2–5 times in the absence of stromal cells and IL-7, whereas the corresponding cells from λ5-deficient mice are unable to proliferate in such conditions, showing that surface expression of a complete pre-BCR is necessary and sufficient to provide constitutive cell signaling (33). Mutations in genes encoding subunits of the pre-BCR and molecules involved in pre-BCR signaling culminate in X-linked and non-X-linked agammaglobulinemia (34). For example, the μHC-affected patients were characterized by a normal level of pro-B cells but an absence of pre-B cells in the BM, and they presented severe hypogammaglobulinemia (35), λ5-, Vpre-B-, and CD79b-deficient mice exhibited a block in B cell development at the pre-B cell stage (20–22), then terminated pre-BCR expression and VJ(L) rearrangement by small pre-B cells destined to become B cells (2). The Btk-null mice also showed a developmental delay of B cells (36). In the present study, in contrast with 70Z/3 cells, the CD79a signaling intensity was attenuated by a factor of 6.7 in 70Z/3-KD cells. Also, in 70Z/3-KD cells, pre-BCR expression on the cell surface was down-regulated by a factor of 5.2 (Fig. 3*A*). It is conceivable that decreased signaling in 70Z/3-KD cells was proportional to the decreased expression of pre-BCR on the cell surface. It is also noteworthy that CD79a phosphorylation was preceded by the sequential activation of Btk at 15 min. The reintroduction of the *Fut8* gene to 70Z/3-KD cells potently rescued pre-BCR-mediated signaling, which was impaired in 70Z/3-KD cells (Fig. 5). In turn, the attenuated signal transduction accounted for the low pre-B cell proliferation in *Fut8*$^{-/-}$ cells and in *Fut8* knockdown cells (Fig. 6). In our previous study, the combined down-regulation of those genes: *CD79a*, *CD79b*, *Ebf1,* and *Tcfe2a*, which promote the activation of B cells, were down-regulated in *Fut8*$^{-/-}$ B progenitors (16). In 12-week-old *Fut8*$^{-/-}$ mice sera, the levels of IgG_1, IgG_{2a}, IgG_{2b}, IgA, IgG3, and IgM were significantly reduced. However, in 2-week-old *Fut8*$^{-/-}$ mice sera, IgG_1, IgG_{2a}, and IgG_{2b} levels were relatively normal, but levels of IgM and IgG_3 were reduced by *Fut8* deficiency, resembling the phenotype of *Btk*$^{-/-}$ mice (38). As to why the levels of IgGs were relatively normal in 2-week-old *Fut8*$^{-/-}$ mice, one possible explanation involves the transfer of IgGs from the pregnant *Fut8*$^{+/-}$ mice through the placenta to the offspring of *Fut8*$^{-/-}$ mice. In our previous study, the existence of core-fucosylated IgG in the serum of early *Fut8*$^{-/-}$ mice was confirmed by mass spectrographic analysis (data not shown).

In conclusion, the phenotype of *Fut8*$^{-/-}$ mice combined with our *in vitro* data presented an intriguing possibility that the core fucose is involved in the appropriate interactions of μHC and λ5, and the assembly of pre-BCR, which is required and sufficient for transduction of pre-BCR intracellular signaling and proliferation. Our results provide insight into the molecular mechanisms of *Fut8*-regulated pre-B cell differentiation and proliferation.

Acknowledgment—We gratefully acknowledge Katsuhiko Ishihara (Kawasaki Medical University, Japan) for critical reading of the manuscript.

REFERENCES

1. Conley, M. E., Rohrer, J., Rapalus, L., Boylin, E. C., and Minegishi, Y. (2000) Defects in early B-cell development: comparing the consequences of abnormalities in pre-BCR signaling in the human and the mouse. *Immunol. Rev.* **178,** 75–90
2. Burrows, P. D., Stephan, R. P., Wang, Y. H., Lassoued, K., Zhang, Z., and Cooper, M. D. (2002) The transient expression of pre-B cell receptors governs B cell development. *Semin. Immunol.* **14,** 343–349
3. Bankovich, A. J., Raunser, S., Juo, Z. S., Walz, T., Davis, M. M., and Garcia, K. C. (2007) Structural insight into pre-B cell receptor function. *Science* **316,** 291–294
4. Espeli, M., Rossi, B., Mancini, S. J., Roche, P., Gauthier, L., and Schiff, C. (2006) Initiation of pre-B cell receptor signaling: common and distinctive features in human and mouse. *Semin. Immunol.* **18,** 56–66
5. Wang, X., Inoue, S., Gu, J., Miyoshi, E., Noda, K., Li, W., Mizuno-Horikawa, Y., Nakano, M., Asahi, M., Takahashi, M., Uozumi, N., Ihara, S., Lee, S. H., Ikeda, Y., Yamaguchi, Y., Aze, Y., Tomiyama, Y., Fujii, J., Suzuki, K., Kondo, A., Shapiro, S. D., Lopez-Otin, C., Kuwaki, T., Okabe, M., Honke, K., and Taniguchi, N. (2005) Dysregulation of TGF-beta1 receptor activation leads to abnormal lung development and emphysema-like phenotype in core fucose-deficient mice. *Proc. Natl. Acad. Sci. U.S.A.* **102,** 15791–15796
6. Li, W., Nakagawa, T., Koyama, N., Wang, X., Jin, J., Mizuno-Horikawa, Y., Gu, J., Miyoshi, E., Kato, I., Honke, K., Taniguchi, N., and Kondo, A. (2006) Down-regulation of trypsinogen expression is associated with growth retardation in alpha1,6-fucosyltransferase-deficient mice: attenuation of proteinase-activated receptor 2 activity. *Glycobiology* **16,** 1007–1019
7. Wang, X., Gu, J., Ihara, H., Miyoshi, E., Honke, K., and Taniguchi, N. (2006) Core fucosylation regulates epidermal growth factor receptor-mediated intracellular signaling. *J. Biol. Chem.* **281,** 2572–2577
8. Shinkawa, T., Nakamura, K., Yamane, N., Shoji-Hosaka, E., Kanda, Y., Sakurada, M., Uchida, K., Anazawa, H., Satoh, M., Yamasaki, M., Hanai,

N., and Shitara, K. (2003) The absence of fucose but not the presence of galactose or bisecting N-acetylglucosamine of human IgG1 complex-type oligosaccharides shows the critical role of enhancing antibody-dependent cellular cytotoxicity. *J. Biol. Chem.* **278,** 3466–3473
9. Pinho, S. S., Seruca, R., Gärtner, F., Yamaguchi, Y., Gu, J., Taniguchi, N., and Reis, C. A. (2011) Modulation of E-cadherin function and dysfunction by N-glycosylation. *Cell Mol. Life Sci.* **68,** 1011–1020
10. Fukuda, T., Hashimoto, H., Okayasu, N., Kameyama, A., Onogi, H., Nakagawasai, O., Nakazawa, T., Kurosawa, T., Hao, Y., Isaji, T., Tadano, T., Narimatsu, H., Taniguchi, N., and Gu, J. (2011) Alpha1,6-fucosyltransferase-deficient mice exhibit multiple behavioral abnormalities associated with a schizophrenia-like phenotype: importance of the balance between the dopamine and serotonin systems. *J. Biol. Chem.* **286,** 18434–18443
11. Ubelhart, R., Bach, M. P., Eschbach, C., Wossning, T., Reth, M., and Jumaa, H. (2010) N-linked glycosylation selectively regulates autonomous precursor BCR function. *Nat. Immunol.* **11,** 759–765
12. Wang, F., Nakouzi, A., Angeletti, R. H., and Casadevall, A. (2003) Site-specific characterization of the N-linked oligosaccharides of a murine immunoglobulin M by high-performance liquid chromatography/electrospray mass spectrometry. *Anal. Biochem.* **314,** 266–280
13. Wright, J. F., Shulman, M. J., Isenman, D. E., and Painter, R. H. (1990) C1 binding by mouse IgM. The effect of abnormal glycosylation at position 402 resulting from a serine to asparagine exchange at residue 406 of the μ-chain. *J. Biol. Chem.* **265,** 10506–10513
14. Haimovich, J., Ben Moshe, N., Raviv, Y., and Hollander, N. (2010) All oligosaccharide moieties of the μ chains in the pre-BCR are of the high-mannose type. *Mol. Immunol.* **48,** 351–355
15. Stubbs, H. J., Lih, J. J., Gustafson, T. L., and Rice, K. G. (1996) Influence of core fucosylation on the flexibility of a biantennary N-linked oligosaccharide. *Biochemistry* **35,** 937–947
16. Li, W., Ishihara, K., Yokota, T., Nakagawa, T., Koyama, N., Jin, J., Mizuno-Horikawa, Y., Wang, X., Miyoshi, E., Taniguchi, N., and Kondo, A. (2008) Reduced alpha4beta1 integrin/vascular cell adhesion molecule-1 interactions lead to impaired pre-B cell repopulation in alpha1,6-fucosyltransferase deficient mice. *Glycobiology* **18,** 114–124
17. Uozumi, N., Teshima, T., Yamamoto, T., Nishikawa, A., Gao, Y. E., Miyoshi, E., Gao, C. X., Noda, K., Islam, K. N., Ihara, Y., Fujii, S., Shiba, T., and Taniguchi, N. (1996) A fluorescent assay method for GDP-L-Fuc:N-acetyl-beta-D-glucosaminide alpha 1–6fucosyltransferase activity, involving high performance liquid chromatography. *J. Biochem.* **120,** 385–392
18. Ishida, H., Moritani, T., Hata, Y., Kawato, A., Suginami, K., Abe, Y., and Imayasu, S. (2002) Molecular cloning and overexpression of fleA gene encoding a fucose-specific lectin of Aspergillus oryzae. *Biosci. Biotechnol. Biochem.* **66,** 1002–1008
19. Miyake, K., Weissman, I. L., Greenberger, J. S., and Kincade, P. W. (1991) Evidence for a role of the integrin VLA-4 in lymphohemopoiesis. *J. Exp. Med.* **173,** 599–607
20. Hess, J., Werner, A., Wirth, T., Melchers, F., Jäck, H. M., and Winkler, T. H. (2001) Induction of pre-B cell proliferation after de novo synthesis of the pre-B cell receptor. *Proc. Natl. Acad. Sci. U.S.A.* **98,** 1745–1750
21. Mårtensson, I. L., Almqvist, N., Grimsholm, O., and Bernardi, A. I. (2010) The pre-B cell receptor checkpoint. *FEBS Lett.* **584,** 2572–2579
22. Kawano, Y., Yoshikawa, S., Minegishi, Y., and Karasuyama, H. (2006) Pre-B cell receptor assesses the quality of IgH chains and tunes the pre-B cell repertoire by delivering differential signals. *J. Immunol.* **177,** 2242–2249
23. Wasserman, R., Li, Y. S., Shinton, S. A., Carmack, C. E., Manser, T., Wiest, D. L., Hayakawa, K., and Hardy, R. R. (1998) A novel mechanism for B cell repertoire maturation based on response by B cell precursors to pre-B receptor assembly. *J. Exp. Med.* **187,** 259–264
24. Cambier, J. C. (1995) Antigen and Fc receptor signaling. The awesome power of the immunoreceptor tyrosine-based activation motif (ITAM). *J. Immunol.* **155,** 3281–3285
25. Partridge, E. A., Le Roy, C., Di Guglielmo, G. M., Pawling, J., Cheung, P., Granovsky, M., Nabi, I. R., Wrana, J. L., and Dennis, J. W. (2004) Regulation of cytokine receptors by Golgi N-glycan processing and endocytosis. *Science* **306,** 120–124
26. Wyss, D. F., Choi, J. S., Li, J., Knoppers, M. H., Willis, K. J., Arulanandam, A. R., Smolyar, A., Reinherz, E. L., and Wagner, G. (1995) Conformation and function of the N-linked glycan in the adhesion domain of human CD2. *Science* **269,** 1273–1278
27. Dwek, R. A. (1995) Glycobiology: more functions for oligosaccharides. *Science* **269,** 1234–1235
28. Rabinovich, E., Bar-Nun, S., Amitay, R., Shachar, I., Gur, B., Taya, M., and Haimovich, J. (1993) Different assembly species of IgM are directed to distinct degradation sites along the secretory pathway. *J. Biol. Chem.* **268,** 24145–24148
29. Corcos, D., Dunda, O., Butor, C., Cesbron, J. Y., Lorès, P., Bucchini, D., and Jami, J. (1995) Pre-B-cell development in the absence of lambda 5 in transgenic mice expressing a heavy-chain disease protein. *Curr. Biol.* **5,** 1140–1148
30. Shaffer, A. L., and Schlissel, M. S. (1997) A truncated heavy chain protein relieves the requirement for surrogate light chains in early B cell development. *J. Immunol.* **159,** 1265–1275
31. Muljo, S. A., and Schlissel, M. S. (2002) The variable, C(H)1, C(H)2 and C(H)3 domains of Ig heavy chain are dispensable for pre-BCR function in transgenic mice. *Int. Immunol.* **14,** 577–584
32. ten Boekel, E., Melchers, F., and Rolink, A. G. (1997) Changes in the V(H) gene repertoire of developing precursor B lymphocytes in mouse bone marrow mediated by the pre-B cell receptor. *Immunity* **7,** 357–368
33. Gauthier, L., Rossi, B., Roux, F., Termine, E., and Schiff, C. (2002) Galectin-1 is a stromal cell ligand of the pre-B cell receptor (BCR) implicated in synapse formation between pre-B and stromal cells and in pre-BCR triggering. *Proc. Natl. Acad. Sci. U.S.A.* **99,** 13014–13019
34. LeBien, T. W. (2000) Fates of human B-cell precursors. *Blood* **96,** 9–23
35. Lopez Granados, E., Porpiglia, A. S., Hogan, M. B., Matamoros, N., Krasovec, S., Pignata, C., Smith, C. I., Hammarstrom, L., Bjorkander, J., Belohradsky, B. H., Casariego, G. F., Garcia Rodriguez, M. C., and Conley, M. E. (2002) Clinical and molecular analysis of patients with defects in micro heavy chain gene. *J. Clin. Invest.* **110,** 1029–1035
36. Middendorp, S., Dingjan, G. M., and Hendriks, R. W. (2002) Impaired precursor B cell differentiation in Bruton's tyrosine kinase-deficient mice. *J. Immunol.* **168,** 2695–2703
37. Winkler, T. H., Rolink, A., Melchers, F., and Karasuyama, H. (1995) Precursor B cells of mouse bone marrow express two different complexes with the surrogate light chain on the surface. *Eur. J. Immunol.* **25,** 446–450
38. Khan, W. N., Alt, F. W., Gerstein, R. M., Malynn, B. A., Larsson, I., Rathbun, G., Davidson, L., Müller, S., Kantor, A. B., Herzenberg, L. A., *et al.* (1995) Defective B cell development and function in Btk-deficient mice. *Immunity* **3,** 283–299